PCCP

PAPER

View Article Online
View Journal | View Issue

Cite this: *Phys. Chem. Chem. Phys.*, 2019, **21**, 24919

Simultaneous enhancement of transition dipole strength and vibrational lifetime of an alkyne IR probe *via* π-d backbonding and vibrational decoupling†

Dorota Kossowska, ‡[ab] Giseong Lee,‡[b] Hogyu Han,*[b] Kyungwon Kwak*[ab] and Minhaeng Cho *[ab]

Alkyne infrared (IR) probes **1–6** with Si and S (or Se) atoms incorporated into the C≡C bond were synthesized, and the vibrational properties of their C≡C stretch mode were studied using Fourier transform infrared (FTIR) and femtosecond IR pump–probe (IR PP) spectroscopies in combination with quantum chemical calculations. From FTIR studies, the transition dipole strengths (in units of 10^{-2} D^2) of **1–3** having the Si atom were measured to be 1.85, 3.32, and 2.52, whereas those of **4–6** having no Si atom were measured to be 0.13, 0.20, and 0.17, respectively, in $CHCl_3$. Thus, the increase in the transition dipole strength of the C≡C stretch mode upon incorporation of the Si atom into the C≡C bond is by a factor of about 14 or higher. The large increase in the transition dipole strength of the C≡C stretch mode upon such Si incorporation is attributed to π-d backbonding between the C≡C group's π and Si atom's d orbitals. From IR PP experiments, the vibrational lifetimes of the C≡C stretch mode in **1–3** having none, S, and Se atoms were determined to be 5.7 ± 0.7, 13.0 ± 1.1, and 94.2 ± 5.8 ps, respectively, in $CHCl_3$. Thus, the increase in the vibrational lifetime of the C≡C stretch mode upon incorporation of the S (or Se) atom between the phenyl ring and the C≡C bond is by a factor of about 2 (or 16) or higher. The large increase in the vibrational lifetime of the C≡C stretch mode upon such S (or Se) incorporation is attributed to its heavy atom effect impeding vibrational couplings between the C≡C stretch and phenyl ring vibrations. From two-dimensional infrared (2DIR) experiments, the large transition dipole strength and long vibrational lifetime of **3** containing the Si and S (or Se) atoms were shown to enable the measurement of its 2DIR spectra up to 500 ps. The strongly absorbing alkynes with long vibrational lifetimes will be a promising probe of molecular dynamics in nonlinear vibrational spectroscopy and imaging on an extended time scale.

Received 6th August 2019,
Accepted 9th October 2019

DOI: 10.1039/c9cp04356j

rsc.li/pccp

Introduction

Infrared (IR) probes have been extensively used as site-specific reporters of the structure, local electric field, hydration, and dynamics of biomolecules.[1–8] Many IR probes much used in Fourier transform infrared (FTIR) studies possess certain desired spectral properties. They often have a spectral signal within the transparent window (~1800–2500 cm^{-1}) free of native signals.[8] They sometimes possess a large transition dipole strength, a narrow bandwidth, and high sensitivity to local structure and environment. Their use in time-resolved nonlinear IR studies is greatly facilitated by two crucially desired spectral properties, namely a large transition dipole strength and long vibrational lifetime. However, IR probes possessing both of these two spectral properties have been rarely explored despite their potential for wide use in two-dimensional infrared (2DIR) studies of biomolecules.

The vibrational lifetime of IR probes can be prolonged by isotopic substitution. The vibrational lifetime of the nitrile (CN) group (<5 ps) increases by about 2-fold upon substitution of $^{12}C^{14}N$ with $^{13}C^{15}N$.[9,10] The vibrational lifetime of IR probes can also be prolonged by the thermal insulation effect of a heavy atom. The vibrational lifetimes of the CN stretch modes of the thiocyanate (SCN) and selenocyanate (SeCN) groups exceed ~50 and ~100 ps, respectively, indicating that the Se atom is more effective than the S atom in increasing the vibrational

[a] *Center for Molecular Spectroscopy and Dynamics, Institute for Basic Science (IBS), Seoul 02841, Korea. E-mail: kkwak@korea.ac.kr, mcho@korea.ac.kr*
[b] *Department of Chemistry, Korea University, Seoul 02841, Korea. E-mail: hogyuhan@korea.ac.kr*

† Electronic supplementary information (ESI) available: Detailed synthetic procedures and characterization for derivatized alkynes; figures and tables showing the additional results of spectroscopic and computational studies. See DOI: 10.1039/c9cp04356j

‡ These two authors contributed equally to this work.

lifetimes of the CN group.[11–16] However, the small transition dipole strength of the CN group ($<1 \times 10^{-2}$ and $<0.4 \times 10^{-2}$ D^2 for aromatic and aliphatic nitriles, respectively[17,18]) remains nearly unchanged upon their isotopic substitution[9,10] and even decreases by about 3-fold upon chalcogenic thermal insulation in aromatic nitriles.[16]

The transition dipole strength of IR probes can be enhanced by stereoelectronic modulation. The transition dipole strength of the isonitrile (NC) group ($>2 \times 10^{-2}$ D^2) is larger than that of the CN group, which is due to the configuration reversal of the atomic electronegativity between the NC and CN groups.[17,18] The transition dipole strength of the CN stretch mode of the cyanamide (NHCN) group is $>3 \times 10^{-2}$ D^2, which is larger than that of the CN and NC groups.[19] The larger transition dipole strength of the NHCN relative to CN group originates from the $n \rightarrow \pi^*$ interaction between the N atom's nonbonding (n) and CN group's antibonding (π^*) orbitals of the NHCN group. However, the vibrational lifetimes of the NC and NHCN groups (<11 and <8 ps, respectively) do not far exceed that of the CN group. The transition dipole strengths of the C≡C stretch mode in $PhSiMe_2CCH$ and *t*-$BuSiMe_2CCH$ are $\sim 1 \times 10^{-2}$ D^2, whereas those in PhCCH and *t*-BuCCH are $\sim 0.1 \times 10^{-2}$ D^2.[20] In addition, the vibrational lifetimes of the C≡C stretch mode in $PhSiMe_2CCH$ and *t*-$BuSiMe_2CCH$ are ~50 ps, whereas those in PhCCH and *t*-BuCCH can hardly be determined because of their very small transition dipole strengths, but they are predicted to be of an order of magnitude similar to the vibrational lifetimes of the CN stretch mode in PhCN and *t*-BuCN. Thus, both the transition dipole strength and vibrational lifetime of the C≡C stretch mode increase by about 10-fold upon insertion of the Si atom between the Ph (or *t*-Bu) and C≡C groups. The simultaneous increase in the two spectral properties of the C≡C stretch mode upon such Si insertion can be attributed to the dual roles of the Si atom. Therein, the Si atom acts as an electronic effector weakening the C≡C bond, *via* π-d back-bonding between the C≡C group's π and Si atom's d orbitals, and as a thermal insulator retarding intramolecular vibrational relaxation (IVR), *via* the heavy atom effect impeding vibrational couplings between the C≡C stretch and Ph ring (or *t*-Bu) vibrations.

Here, we report novel IR probes based on alkynes containing the Si and S (or Se) atoms covalently bonded to the C atoms of the C≡C bond. These alkyne IR probes are designed to have their transition dipole strengths and vibrational lifetimes modulated by Si and S (or Se) atoms, respectively. The comparative IR studies of alkynes **1–6** (X–C≡C–Y, where X = Ph, PhS, or PhSe, Y = $SiMe_3$ or H, Fig. 1) show that the transition dipole strengths and vibrational lifetimes of the C≡C stretch mode increase by more than 14-fold and 2-fold (or 16-fold) upon incorporation of the Si and S (or Se) atoms into the C≡C bond, respectively. The results suggest a new design principle for alkyne IR probes, whereby the increase in their transition dipole strengths and vibrational lifetimes can be modulated by the Si and S (or Se) atoms, respectively, independent of each other. Such alkyne IR probes will be of great use in nonlinear vibrational spectroscopy and imaging on an extended time scale.

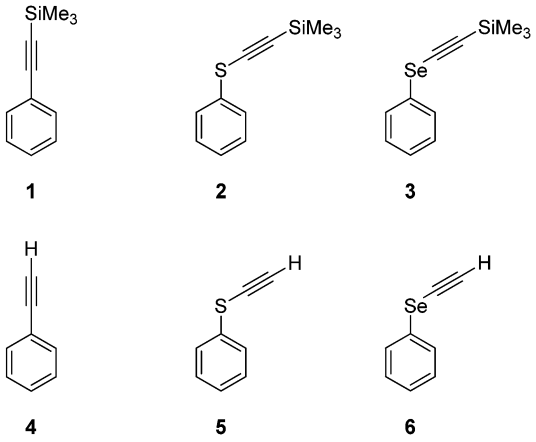

Fig. 1 Structures of alkyne IR probes **1–6**.

Experimental and computational methods

Materials

Compounds **2**, **3**, **5**, and **6** were synthesized and characterized (Scheme 1 and Section SI of the ESI†). Compound **1** was purchased from Alfa Aesar. Compound **4** and all solvents for IR spectroscopy were purchased from Sigma-Aldrich and used as received.

IR spectroscopies

FTIR, polarization-controlled IR pump–probe, and 2DIR experiments were performed as described previously.[20]

Quantum chemical calculations

The *ab initio* calculations for the six model systems, X–C≡C–Y (X = Ph, PhS, or PhSe, Y = $SiMe_3$ or H), were performed using the Kohn–Sham formulation of density functional theory (DFT). The B3LYP (Becke, three-parameter, Lee–Yang–Parr)[21,22] exchange–correlation functional and 6-311++G** basis set were utilized for geometry optimizations, and subsequent harmonic frequency and natural bond orbital (NBO) calculations. All calculations were performed using the GAUSSIAN 09 suite of programs.[23]

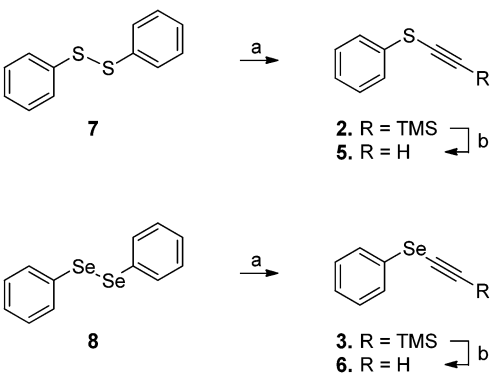

Scheme 1 Syntheses of **2**, **3**, **5** and **6**.[a] [a] *Reagents and conditions*: (a) TMSCCH, *n*-BuLi, THF, −78 °C and then rt, (**2**, 89%; **5**, 91%); (b) K_2CO_3, MeOH, rt, (**3**, 77%; **6**, 57%).

Results and discussion

To obtain information about the solvatochromic behaviors of alkynes, the FTIR spectra of **1–6** in the C≡C stretch region were investigated with various solvents (Fig. 2). The results of the detailed spectral analyses are given in Table 1 and Tables S1–S3 of the ESI.† The molar extinction spectra of **1–6** in $CHCl_3$ are shown in Fig. 2a, and the numerical values of the extinction coefficients and transition dipole strengths are given in Table 1. The most striking feature of the spectra is that each of the trimethylsilyl (TMS)-derivatized alkynes **1–3** gives a very intense absorption band in comparison to the underivatized analogs **4–6**. The transition dipole strengths (in units of 10^{-2} D^2) of **1–6** are 1.85, 3.32, 2.52, 0.13, 0.20, and 0.17, respectively. Thus, the increase in the transition dipole strength of the C≡C stretch mode upon incorporation of the TMS group into the C≡C bond is by more than 14 times (their ratio is 14.2 between **1** and **4**, 16.6 between **2** and **5**, and 14.8 between **3** and **6**). However, such an increase upon incorporation of the PhS (or PhSe) group into the C≡C bond is by less than 2 times (their ratio is 1.8 between **1** and **2**, 1.4 between **1** and **3**, 1.5 between **4** and **5**, and 1.3 between **4** and **6**). Thus, the increase in the transition dipole strength of the C≡C stretch mode is caused primarily by the TMS rather than PhS (or PhSe) group. Note that the transition dipole strength of the CN group is $<1 \times 10^{-2}$ and $<0.4 \times 10^{-2}$ D^2 for aromatic and aliphatic nitriles,[17,18] which decreases by about 3-fold and increases by about 4-fold upon incorporation of the S (or Se) atom into the C≡N bond, respectively.[16,24] Thus, the transition dipole strengths of the TMS-derivatized alkynes are larger than those of the CN, SCN,

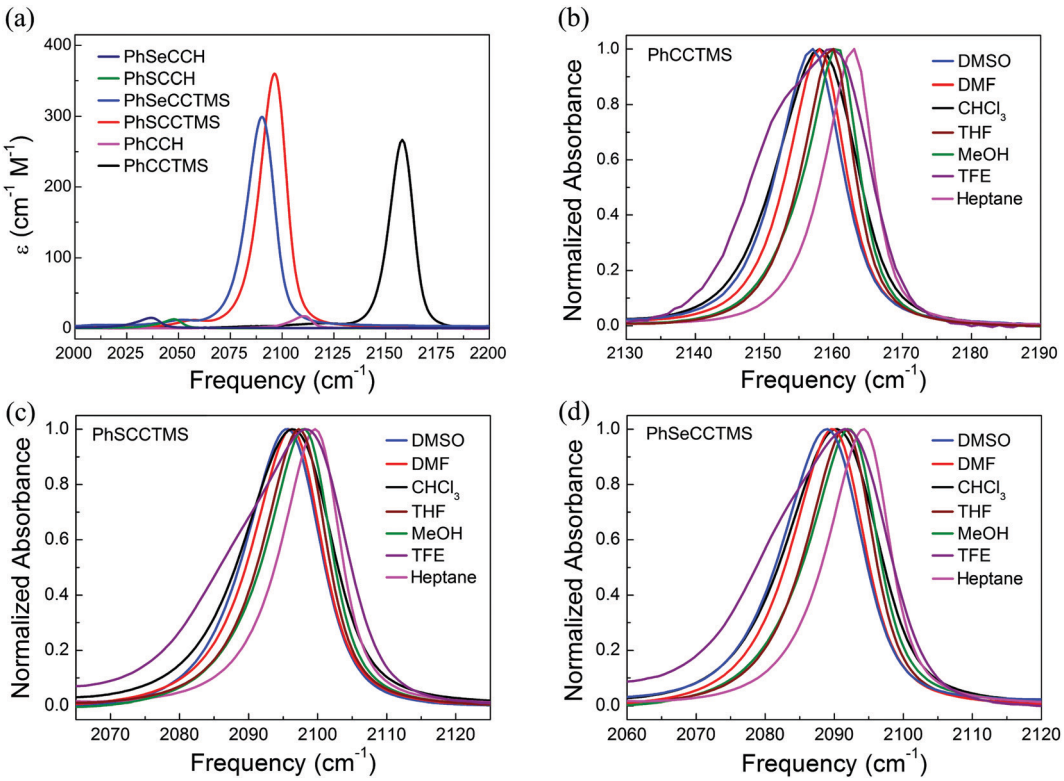

Fig. 2 (a) Molar extinction spectra of **1–6** in $CHCl_3$. (b–d) Normalized FTIR spectra of **1–3** in various solvents. TFE stands for 2,2,2-trifluoroethanol. For spectral analyses, see Tables S1–S3 of the ESI.†

Table 1 Experimentally measured and theoretically calculated spectral properties of **1–6**[a]

		PhCCTMS	PhSCCTMS	PhSeCCTMS	PhCCH	PhSCCH	PhSeCCH
Experiment	ω_0 (cm^{-1})	2157.5	2095.3	2089.6	2109.1	2046.4	2035.3
	FWHM (cm^{-1})	13.0	15.2	15.5	12.3	12.5	13.1
	ε (cm^{-1} M^{-1})	266.7	360.0	299.1	17.5	13.0	15.0
	D (10^{-2} D^2)[b]	1.85	3.32	2.52	0.13	0.20	0.17
	T_1 (ps)	5.7 ± 0.7	13.0 ± 1.1	94.2 ± 5.8	—	—	—
Theory	ω_0 (cm^{-1})[c]	2171.3	2106.0	2098.6	2128.9	2063.7	2051.6
	I_{IR} (D^2/(amu Å^2))[d]	2.29	3.81	2.95	0.25	0.63	0.36
	CC bond length (Å)	1.2161	1.2192	1.2193	1.2050	1.2074	1.2077

[a] Fitting parameters obtained from the Voigt fitting analysis of the FTIR spectra shown in Fig. 2a (ω_0, FWHM, ε, and D) and the single-exponential-fitting analysis of the IR pump–probe signal decays shown in Fig. 4a (T_1). [b] Ref. 35. [c] A scaling factor of 0.9670 was used. [d] IR intensity.

and SeCN groups. As will be shown later, the transition dipole strengths of the TMS-derivatized alkynes are large enough to give the high-quality IR pump–probe and 2DIR spectra, which are hard to obtain for aliphatic nitriles, thiocyanates, and selenocyanates. Note that the transition dipole strength of the C≡C group increases in aromatic alkynes, whereas that of the C≡N group decreases in aromatic nitriles and increases in aliphatic nitriles upon incorporation of the S (or Se) atom into these triple bonds.

To obtain information about the ability of alkynes to quantitatively report on the local electric field or the interaction energy between the solute and solvent molecules, the FTIR spectra of **1–3** were measured in a variety of nonpolar (heptane, hexane, and $CHCl_3$), polar aprotic (DMSO, DMF, THF, and $CH_3CO_2CH_3$), and polar protic solvents (2,2,2-trifluoroethanol (TFE) and CH_3OH) (Fig. 2b–d). The spectra of **1–3** in all the solvents except for TFE exhibit a singlet with a slight elongation to the low-frequency side. This small asymmetry of the spectral line shape is, however, less pronounced than that in the case of **4–6**. The spectra of **1–3** in TFE, the strongest H-bond donor among the solvents considered here,[25] exhibit a doublet with the low- and high-frequency peaks assigned to the C≡C stretch mode of their non-H-bonded and H-bonded species, respectively. All of the spectra were fitted to the Voigt function and the fitting parameters are given in Table 1 and Tables S1–S3 of the ESI.† The C≡C stretch spectra of **1–3** in nonpolar and polar solvents used here exhibit small solvent-dependent frequency shifts of just 4.4–5.8 cm^{-1} and narrow bandwidths (full width at half-maximum (FWHM)) of <16 cm^{-1}. The lowest frequency peak was observed in DMSO, DMF, and $CHCl_3$, whereas the highest frequency peak was observed in heptane. The frequency dependence of the C≡C stretch mode on the dielectric constant ε and Kamlet–Taft parameters α and β[26] of the solvents for **1–3** is shown in Fig. S1 of the ESI.† Note that the C≡C stretch frequencies are red-shifted by about 50 and 60 (or 70) cm^{-1} upon incorporation of the Si and S (or Se) atoms to the C≡C bond, respectively. Similar frequency red-shifts of about 30 and 90 (or 100) cm^{-1} were observed for the C≡N stretch mode upon incorporation of the NH group[19] and S (or Se) atom[11,14,16] into the C≡N bond. Thus, the frequency red-shift of the C≡C stretch mode is smaller than that of the C≡N stretch mode upon incorporation of the S (or Se) atoms into these triple bonds.

To explain the large increase in the transition dipole strength of the C≡C stretch mode upon incorporation of the TMS group into the C≡C bond, we next studied the influence of the Si atom on the vibrational properties of the C≡C group. For this purpose, we performed vibrational and NBO analyses for **1–6** as model molecules using DFT calculations (Fig. S2 of the ESI†). The results of the vibrational analysis are given in Table 1. The calculated vibrational frequencies of the C≡C stretch mode were quite close to the experimentally measured ones within an error of 1%. The trends in the Si- and S (or Se)-induced frequency shifts of the C≡C stretch mode and the large Si-induced increase in its transition dipole strength match quite well between the calculated and experimental data. The results of the NBO analysis

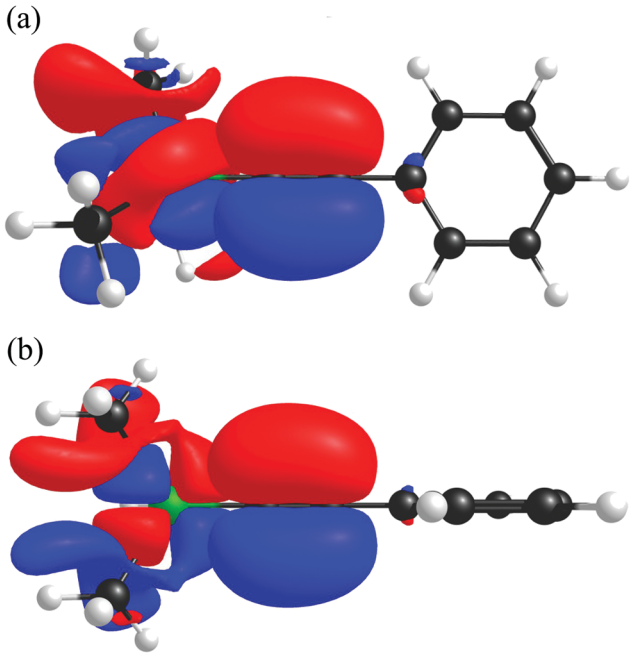

Fig. 3 π-d backbonding between the C≡C group's π and Si atom's d orbitals in **1**: (a) Si d_{yz} and C≡C π_y, (b) Si d_{xz} and C≡C π_x. The C≡C bond is along the z-axis.

are shown in Fig. 3 and Table S4 of the ESI.† The large increase in the transition dipole strength of the C≡C stretch mode upon incorporation of the Si atom into the C≡C bond can be understood by noting π-d backbonding between the C≡C group's π and Si atom's d orbitals.[27–29] The π-d orbital overlap occurs in two planes parallel and perpendicular to the phenyl ring. Such π-d backbonding strengthens the C–Si bond between the C≡C group and the Si atom and weakens the C≡C bond. The weakening of the C≡C bond upon such π-d backbonding leads to the increase in the C≡C bond length and hence the transition dipole strength of the C≡C stretch mode. A clear correlation between the C≡C bond length and the transition dipole strength of the C≡C stretch mode is shown in Table 1. The weakening of the C≡C bond upon such π-d backbonding causes the red-shift of its vibrational frequency.

The small increase in the transition dipole strength of the C≡C group and its frequency red-shift in aromatic alkynes upon incorporation of the S (or Se) atom between the phenyl ring and the C≡C bond could be understood by noting just two orbital–orbital interactions: (1) the π (π*) → π* interaction between the phenyl ring's π (π*) and C≡C group's π* orbitals; (2) the n → π* interaction between the S (or Se) atom's n and C≡C group's π* orbitals.[19] Upon such S (or Se) incorporation, the π (π*) → π* interaction is broken and the n → π* interaction is made. Both interactions weaken the C≡C bond, which leads to the increase in the C≡C bond length and hence the transition dipole strength of the C≡C stretch mode. The weakening of the C≡C bond upon such π (π*) → π* and n → π* interactions causes the red-shift of its vibrational frequency. The stabilization energy of the n → π* interaction was calculated to be larger than that of the π (π*) → π* interaction for the C≡C

group in aromatic alkynes (data not shown). Thus, the increase in the transition dipole strength of the C≡C group and its frequency red-shift in aromatic alkynes upon such S (or Se) incorporation could be attributed to the stronger n → π* relative to π (π*) → π* interaction. The stabilization energy of the n → π* interaction was also calculated to be larger than that of the π (π*) → π* interaction for the C≡N group in aromatic nitriles (data not shown). However, the decrease in the transition dipole strength of the C≡N group unlike its frequency red-shift in aromatic nitriles upon such S (or Se) incorporation cannot be accounted for by the stronger n → π* relative to π (π*) → π* interaction. The stabilization energies of the π (π*) → π* and n → π* interactions were calculated to be similar between the C≡C and C≡N groups in aromatic alkynes and nitriles (data not shown). However, the smaller frequency red-shift of the C≡C group compared to that of the C≡N group in aromatic alkynes and nitriles upon such S (or Se) incorporation cannot be accounted for by the similarly stronger n → π* relative to π (π*) → π* interaction. Taken together, the effect of such S (or Se) incorporation on the transition dipole strength of the C≡C and C≡N groups and their frequency red-shift in aromatic alkynes and nitriles cannot be accounted for by considering only these two orbital–orbital interactions and it needs to be addressed by further study in the future.

To determine the vibrational lifetimes of the C≡C stretch mode in alkyne probes, the polarization-controlled IR pump–probe (IR PP) measurements of **1–3** were performed. The IR PP spectrum consists of a high-frequency positive peak arising from a ground-state bleach ($\nu = 0 \rightarrow 1$ transition) and stimulated emission ($\nu = 1 \rightarrow 0$ transition), and a low-frequency negative peak arising from excited-state absorption ($\nu = 1 \rightarrow 2$ transition). To obtain the vibrational lifetimes, the frequency-dependent slices of the IR PP signals in the region of positive and negative peaks were fitted to a single-exponential decay function and then the resulting frequency-dependent vibrational lifetimes were averaged. The IR PP data analyses of **1–3** in $CHCl_3$ are shown in Fig. 4a, Table 1, and Table S5 of the ESI.† The vibrational lifetimes of the C≡C stretch mode in **1–3** were determined to be 5.7 ± 0.7, 13.0 ± 1.1, and 94.2 ± 5.8 ps, respectively. Thus, the increase in the vibrational lifetime of the C≡C stretch mode upon incorporation of the S (or Se) atom between the phenyl ring and the C≡C bond is more than 2 (or 16) times. The large increase in the vibrational lifetime of the C≡C stretch mode upon such S (or Se) incorporation can be understood by noting its heavy atom effect[11,14,16] impeding vibrational couplings between the C≡C stretch and phenyl ring vibrations. Such a heavy atom effect retards intramolecular vibrational relaxation (IVR). The S (or Se) incorporation between the phenyl ring and the C≡C bond increases the vibrational lifetime of the C≡C stretch mode without causing the decrease in its transition dipole strength. This is in contrast to the case of the C≡N stretch mode, where the S (or Se) incorporation between the phenyl ring and the C≡N bond increases its vibrational lifetime but causes the decrease in its transition dipole strength. Thus, the S (or Se) atom acts as a thermal insulator, increasing the vibrational lifetime of the C≡C stretch mode without diminishing its transition dipole strength. The Si incorporation increases the transition dipole strength of the C≡C stretch mode without causing a decrease in its vibrational lifetime. Thus, the Si atom acts as an electronic effector, increasing the transition dipole strength of the C≡C stretch mode without shortening its vibrational lifetime. Consequently, the Si and S (or Se) atoms on the opposite side of the C≡C bond act as modulators, increasing the transition dipole strength and vibrational lifetime of the C≡C stretch mode, respectively, independent of each other.

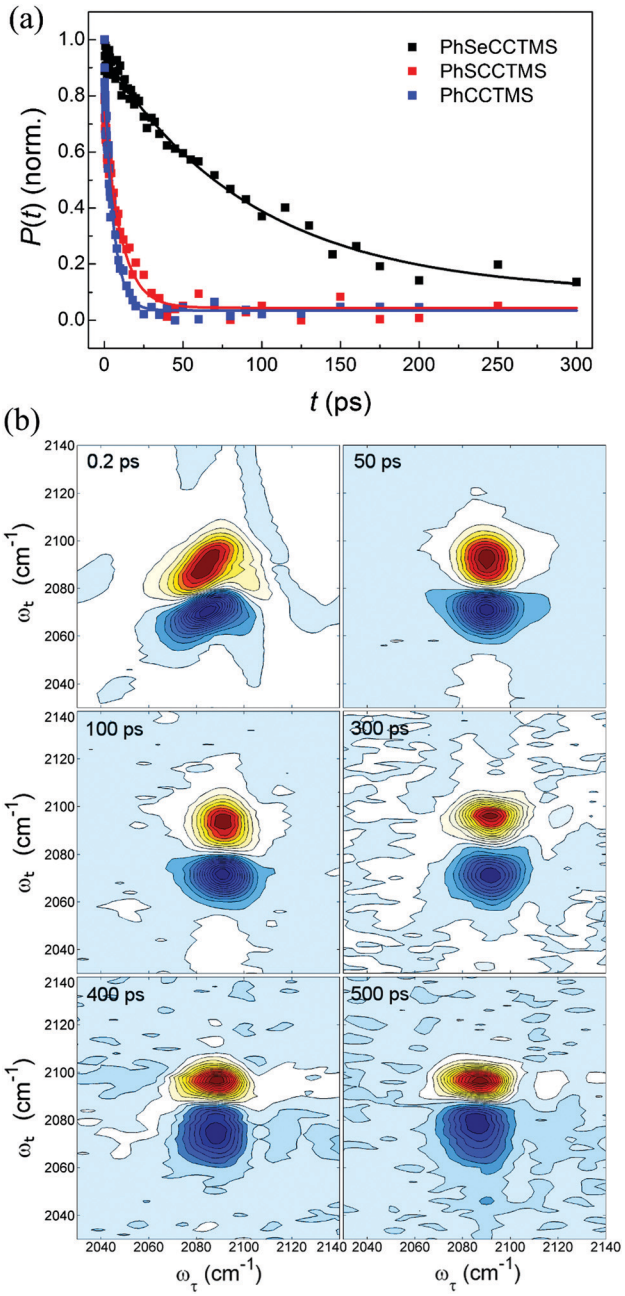

Fig. 4 (a) Vibrational population decays of **1–3** in $CHCl_3$. The plots for **1–3** were obtained from the slices of the IR PP signals (Fig. S3 of the ESI†) at the probe frequencies of 2160.0, 2095.5, and 2097.2 cm^{-1}, respectively. (b) 2DIR spectra of **3** in $CHCl_3$ at various waiting times (T_ws) of 0.2–500 ps.

To evaluate the potential of alkynes as an IR probe of molecular dynamics in nonlinear vibrational spectroscopy, 2DIR experiments of **3** were performed. The 2DIR spectrum reports on the correlation between the initially excited (ω_τ) and finally detected (ω_t) vibrational frequencies of the system at a given waiting time (T_w).[2,16] The 2DIR spectrum contains a positive peak arising from a ground-state bleach ($\nu = 0 \rightarrow 1$ transition) and stimulated emission ($\nu = 1 \rightarrow 0$ transition) along the diagonal ($\omega_\tau = \omega_t$), and a negative peak arising from excited-state absorption ($\nu = 1 \rightarrow 2$ transition) below the diagonal ($\omega_\tau > \omega_t$). A set of 2DIR spectra taken at various T_ws in $CHCl_3$ is shown in Fig. 4b. The positive and negative peaks are separated by the anharmonic shift, $\Delta = \sim 20\ cm^{-1}$. At short $T_w = 0.2$ ps, the two peaks are elongated along the diagonal, which reflects the inhomogeneity in frequencies caused by interaction between the C≡C oscillator and the solvent molecules. With increasing T_w, the spectra become less elongated, which is due to the fluctuation of the solute–solvent interactions. At $T_w = 50$ and 100 ps, the spectra are symmetrical and the positive peak is almost circular. At longer $T_w = 300$–500 ps, the spectra are symmetrical but the positive peak is slightly flattened. Thus, the good-quality 2DIR spectra were obtained up to $T_w = 500$ ps, and can be obtained at longer $T_w > 500$ ps unless the mechanical delay stage generates the pulse delays of only up to 500 ps. Consequently, the large transition dipole strength and long vibrational lifetime of an alkyne containing the Si and S (or Se) atoms make it a promising 2DIR probe on an extended time scale of up to a nanosecond.

Summary

In the present work, we studied the vibrational properties of alkyne IR probes **1–6** using FTIR and ultrafast IR pump–probe methods in combination with quantum chemical calculations. First of all, the transition dipole strength and vibrational lifetime of the C≡C stretch mode increase by more than 14-fold and 2-fold (or 16-fold) upon incorporation of the Si and S (or Se) atoms into the C≡C bond, respectively. The large increase in the transition dipole strength of the C≡C stretch mode upon such Si incorporation is attributed to π-d backbonding between the C≡C group's π and Si atom's d orbitals. The large increase in the vibrational lifetime of the C≡C stretch mode upon such S (or Se) incorporation is attributed to its heavy atom effect impeding vibrational couplings between the C≡C stretch and phenyl ring vibrations. The large transition dipole strength and long vibrational lifetime of **3** containing the Si and Se atoms enable 2DIR experiments to be carried out up to 500 ps. Such alkyne probes will be of great use for studying the structure and dynamics of complicated molecular systems in condensed phases with time-resolved IR spectroscopic techniques as well as for imaging studies of biomolecules in living cells with coherent Raman scattering and linear and nonlinear IR microscopic methods.[30–34]

Conflicts of interest

There are no conflicts to declare.

Acknowledgements

This work was supported by IBS-R023-D1. H. H. is grateful for the financial support from the National Research Foundation (NRF) of Korea funded by the Ministry of Science and ICT (NRF2016R1A2B4013572 and NRF2019R1H1A2079948).

References

1 M. H. Cho, Coherent Two-Dimensional Optical Spectroscopy, *Chem. Rev.*, 2008, **108**, 1331–1418.
2 A. L. Le Sueur, R. E. Horness and M. C. Thielges, Applications of Two-Dimensional Infrared Spectroscopy, *Analyst*, 2015, **140**, 4336–4349.
3 A. Ghosh, J. S. Ostrander and M. T. Zanni, Watching Proteins Wiggle: Mapping Structures with Two-Dimensional Infrared Spectroscopy, *Chem. Rev.*, 2017, **117**, 10726–10759.
4 M. M. Waegele, R. M. Culik and F. Gai, Site-Specific Spectroscopic Reporters of the Local Electric Field, Hydration, Structure, and Dynamics of Biomolecules, *J. Phys. Chem. Lett.*, 2011, **2**, 2598–2609.
5 H. Kim and M. Cho, Infrared Probes for Studying the Structure and Dynamics of Biomolecules, *Chem. Rev.*, 2013, **113**, 5817–5847.
6 J. Ma, I. M. Pazos, W. Zhang, R. M. Culik and F. Gai, Site-Specific Infrared Probes of Proteins, *Annu. Rev. Phys. Chem.*, 2015, **66**, 357–377.
7 P. M. Gosavi and I. V. Korendovych, Minimalist IR and Fluorescence Probes of Protein Function, *Curr. Opin. Chem. Biol.*, 2016, **34**, 103–109.
8 R. Adhikary, J. Zimmermann and F. E. Romesberg, Transparent Window Vibrational Probes for the Characterization of Proteins With High Structural and Temporal Resolution, *Chem. Rev.*, 2017, **117**, 1927–1969.
9 J. M. Rodgers, W. Zhang, C. G. Bazewicz, J. Chen, S. H. Brewer and F. Gai, Kinetic Isotope Effect Provides Insight into the Vibrational Relaxation Mechanism of Aromatic Molecules: Application to Cyano-phenylalanine, *J. Phys. Chem. Lett.*, 2016, **7**, 1281–1287.
10 A. L. Le Sueur, S. Ramos, J. D. Ellefsen, S. Cook and M. C. Thielges, Evaluation of *p*-(^{13}C,^{15}N-Cyano)phenylalanine as an Extended Time Scale 2D IR Probe of Proteins, *Anal. Chem.*, 2017, **89**, 5254–5260.
11 K.-H. Park, J. Jeon, Y. Park, S. Lee, H.-J. Kwon, C. Joo, S. Park, H. Han and M. Cho, Infrared Probes Based on Nitrile-Derivatized Prolines: Thermal Insulation Effect and Enhanced Dynamic Range, *J. Phys. Chem. Lett.*, 2013, **4**, 2105–2110.
12 K. P. Sokolowsky and M. D. Fayer, Dynamics in the Isotropic Phase of Nematogens Using 2D IR Vibrational Echo Measurements on Natural-Abundance ^{13}CN and Extended Lifetime Probes, *J. Phys. Chem. B*, 2013, **117**, 15060–15071.
13 M. Maj, K. Kwak and M. Cho, Ultrafast Structural Fluctuations of Myoglobin-Bound Thiocyanate and Selenocyanate Ions Measured with Two-Dimensional Infrared Photon Echo Spectroscopy, *ChemPhysChem*, 2015, **16**, 3468–3476.
14 D. E. Levin, A. J. Schmitz, S. M. Hines, K. J. Hines, M. J. Tucker, S. H. Brewer and E. E. Fenlon, Synthesis and

Evaluation of the Sensitivity and Vibrational Lifetimes of Thiocyanate and Selenocyanate Infrared Reporters, *RSC Adv.*, 2016, **43**, 36231–36237.

15 S. A. Yamada, H. E. Bailey, A. Tamimi, C. Li and M. D. Fayer, Dynamics in a Room-Temperature Ionic Liquid from the Cation Perspective: 2D IR Vibrational Echo Spectroscopy, *J. Am. Chem. Soc.*, 2017, **139**, 2408–2420.

16 S. Ramos, K. J. Scott, R. E. Horness, A. L. Le Sueur and M. C. Thielges, Extended Timescale 2D IR Probes of Proteins: *p*-Cyanoselenophenylalanine, *Phys. Chem. Chem. Phys.*, 2017, **19**, 10081–10086.

17 M. Maj, C. Ahn, D. Kossowska, K. Park, K. Kwak, H. Han and M. Cho, β-Isocyanoalanine as an IR probe: Comparison of Vibrational Dynamics between Isonitrile and Nitrile-Derivatized IR Probes, *Phys. Chem. Chem. Phys.*, 2015, **17**, 11770–11778.

18 M. Maj, C. Ahn, B. Błasiak, K. Kwak, H. Han and M. Cho, Isonitrile as an Ultrasensitive Infrared Reporter of Hydrogen-Bonding Structure and Dynamics, *J. Phys. Chem. B*, 2016, **120**, 10167–10180.

19 G. Lee, D. Kossowska, J. Lim, S. Kim, H. Han, K. Kwak and M. Cho, Cyanamide as an Infrared Reporter: Comparison of Vibrational Properties between Nitriles Bonded to N and C Atoms, *J. Phys. Chem. B*, 2018, **122**, 4035–4044.

20 D. Kossowska, K. Park, J. Y. Park, C. Lim, K. Kwak and M. Cho, Rational Design of an Acetylenic Infrared Probe with Enhanced Dipole Strength and Increased Vibrational Lifetime, *J. Phys. Chem. B*, 2019, **123**, 6274–6281.

21 A. D. Becke, Density-Functional Exchange-Energy Approximation with Correct Asymptotic Behavior, *Phys. Rev. A: At., Mol., Opt. Phys.*, 1988, **38**, 3098–3100.

22 C. Lee, W. Yang and R. G. Parr, Development of the Colle-Salvetti Correlation-Energy Formula into a Functional of the Electron Density, *Phys. Rev. B: Condens. Matter Mater. Phys.*, 1988, **37**, 785–789.

23 M. J. Frisch, G. W. Trucks, H. B. Schlegel, G. E. Scuseria, M. A. Robb, J. R. Cheeseman, G. Scalmani, V. Barone, B. Mennucci and G. A. Petersson, *et al.*, *Gaussian 09, revision E.01*, Gaussian, Inc., Wallingford, CT, 2009.

24 K.-I. Oh, J.-H. Lee, C. Joo, H. Han and M. Cho, β-Azidoalanine as an IR Probe: Application to Amyloid Aβ(16-22) Aggregation, *J. Phys. Chem. B*, 2008, **112**, 10352–10357.

25 M. Heger, T. Scharge and M. A. Suhm, From Hydrogen Bond Donor to Acceptor: the Effect of Ethanol Fluorination on the First Solvating Water Molecule, *Phys. Chem. Chem. Phys.*, 2013, **15**, 16065–16073.

26 M. J. Kamlet, J.-L. M. Abboud, M. H. Abraham and R. W. Taft, Linear Solvation Energy Relationships. 23. A Comprehensive Collection of the Solvatochromic Parameters, π*, α, and β, and Some Methods for Simplifying the Generalized Solvatochromic Equation, *J. Org. Chem.*, 1983, **48**, 2877–2887.

27 R. West and C. S. Kraihanzel, Infrared Spectral Evidence for Dative π-Bonding in Ethynylsilanes, *Inorg. Chem.*, 1962, **1**, 967–969.

28 H. Bock and H. Seidl, d-Orbital Effects in Silicon Substituted π-Electron Systems. Part XII. Some Spectroscopic Properties of Alkyl and Silyl Acetylenes and Polyacetylenes, *J. Chem. Soc. B*, 1968, 1158–1163.

29 H. Bock and H. Alt, d-Orbitaleffekte in Silicium-substituierten π-Elektronensystemen, XXV. Eigenschaftsunterschiede R_3Si-, R_3C- und R_3SiCH_2-substituierter Phenylacetylene, *Chem. Ber.*, 1970, **103**, 1784–1791.

30 H. Yamakoshi, K. Dodo, M. Okada, J. Ando, A. Palonpon, K. Fujita, S. Kawata and M. Sodeoka, Imaging of EdU, an Alkyne-Tagged Cell Proliferation Probe, by Raman Microscopy, *J. Am. Chem. Soc.*, 2011, **133**, 6102–6105.

31 L. Wei, F. Hu, Y. Shen, Z. Chen, Y. Yu, C.-C. Lin, M. C. Wang and W. Min, Live-Cell Imaging of Alkyne-Tagged Small Biomolecules by Stimulated Raman Scattering, *Nat. Methods*, 2014, **11**, 410–412.

32 X. Li, M. Jiang, J. W. Y. Lam, B. Z. Tang and J. Y. Qu, Mitochondrial Imaging with Combined Fluorescence and Stimulated Raman Scattering Microscopy Using a Probe of the Aggregation-Induced Emission Characteristic, *J. Am. Chem. Soc.*, 2017, **139**, 17022–17030.

33 J.-X. Cheng and X. S. Xie, *Coherent Raman Scattering Microscopy*, CRC Press, Boca Raton, 2018.

34 M. Cho, *Coherent Multidimensional Spectroscopy*, Springer, Singapore, 2019.

35 X. Qu, E. Lee, G.-S. Yu, T. B. Freedman and L. A. Nafie, Quantitative Comparison of Experimental Infrared and Raman Optical Activity Spectra, *Appl. Spectrosc.*, 1996, **50**, 649–657.